Optimal spike-based communication in excitable networks with strong-sparse and weak-dense links

Jun-nosuke Teramae[1,4], Yasuhiro Tsubo[1] and Tomoki Fukai[1,2,3]

[1]RIKEN Brain Science Institute, 2-1 Hirosawa, Wako, Saitama 351-0198, Japan

[2]Brain and Neural Systems Team, RIKEN Computational Science Research Program, 2-1 Hirosawa, Wako, Saitama, 351-0198, Japan

[3]CREST, JST, 4-1-8 Honcho, Kawaguchi, Saitama 332-0012, Japan

[4]PRESTO, JST, 4-1-8 Honcho, Kawaguchi, Saitama 332-0012, Japan

Supplementary Methods

Gaussian-connected network model

The Gaussian-connected network is the same as the SSWD network except that the amplitudes of EPSPs on excitatory neurons were randomly drawn from a Gaussian distribution. The amplitudes were redrawn until positive values were obtained for all synapses. Thus obtained EPSPs obey a truncated Gaussian distribution without a negative portion. Considering both effects of the truncation and failure rate of synaptic transmissions, we can calculate the mean and variance of the truncated Gaussian distribution of EPSPs by numerically solving the following equations:

$$\begin{cases} \int_0^\infty N(x;\mu,\sigma)\frac{ax}{a+x}dx = \int_0^\infty P(x)\frac{ax}{a+x}dx \\ \int_0^\infty N(x;\mu,\sigma)\frac{ax^2}{a+x}dx = \int_0^\infty P(x)\frac{ax^2}{a+x}dx \end{cases},$$

where $N(x; \mu, \sigma)$ is the density function of the Gaussian distribution with mean μ and SD σ.

Electrophysiology

All experiments were performed in accordance with animal protocols approved by the Experimental Animal Committee of the RIKEN Institute. Sagittal cortical slices (400μm thick) were prepared from sensorimotor cortex of Wistar rats (P17 to P25), using a

micro-slicer (PRO-7; Dosaka, Kyoto, Japan) after deep anaesthesia with diethyl ether gas. Whole-cell patch-clamp recordings were performed in a submerged-type recording chamber at 32 °C in circulated normal artificial CSF (ACSF) containing (in mM) 124 NaCl, 2.5 KCl, 1.2 $MgSO_4$, 1.2 KH_2PO_4, 26 $NaHCO_3$, 2.5 $CaCl_2$ and 25 D-glucose, and was saturated with 95% O_2 and 5% CO_2 gas [28,29]. To block the spontaneous synaptic input via AMPA, NMDA and GABAA receptors, 6-cyano-7-nitroquinoxaline-2,3 dione (CNQX; 20μM), DL-2-amino-5-phosphonopentanoic acid (DL-AP5; 25μM) and bicuculline methiodide (BMI; 10μM) were added respectively to the ACSF and bath-applied to the cortical slices. All three antagonists were purchased from Sigma (St. Louis, MO). Spike responses to the fluctuating conductance input were recorded from pyramidal neurons (mainly layer 5) using whole-cell patch pipettes filled with (in mM) 140 K-gluconate, 2 NaCl, 1 $MgCl_2$, 10 HEPES, 0.2 EGTA, 2 5'-$ATPNa_2$, 0.5 $GTPNa_2$ and 10 biocytin (pH 7.4). We used an Axoclamp 2B amplifier (Molecular Devices, Union City, CA) in a conventional bridge mode and a Digidata 1322A analog/digital interface (Molecular Devices) for data acquisition at 50 kHz. In each trial, a fluctuating conductance input described by Equation 2 was injected for 10 s using the dynamic-clamp technique by an analog-type real-time conductance injection amplifier (SM-1; Cambridge Conductance, Cambridge, UK). Trials were separated by more than 20 s inter-trial intervals. For each parameter set, three to six trials were repeated by using different seeds for random number generation. The average and standard error of the cross correlations for these trials were plotted in Fig. 1c and 1d.

Precise spike sequences

W sought precise spike sequences by utilizing our priori knowledge of the underling circuit structure. For a randomly generated long-tailed network, we identified pairs of neurons connected by extremely strong EPSPs (> 8 mV) as candidate pathways through which precise spike sequences may repeatedly propagate. By performing numerical simulations on the network, we constructed spike cross-correlograms for these neuron

pairs (Figure 3d shows their average over all the neuron pairs). A higher peak of the cross-correlogram indicates a more frequent activation of the same pre- and post-synaptic neuron pair within short delays. Therefore, we selected such neuron pairs that exhibit extremely significant peaks (> 100 Hz). We then searched connected paths by Depth First Search algorithm and represented precise sequences as links connecting the neuron pairs.

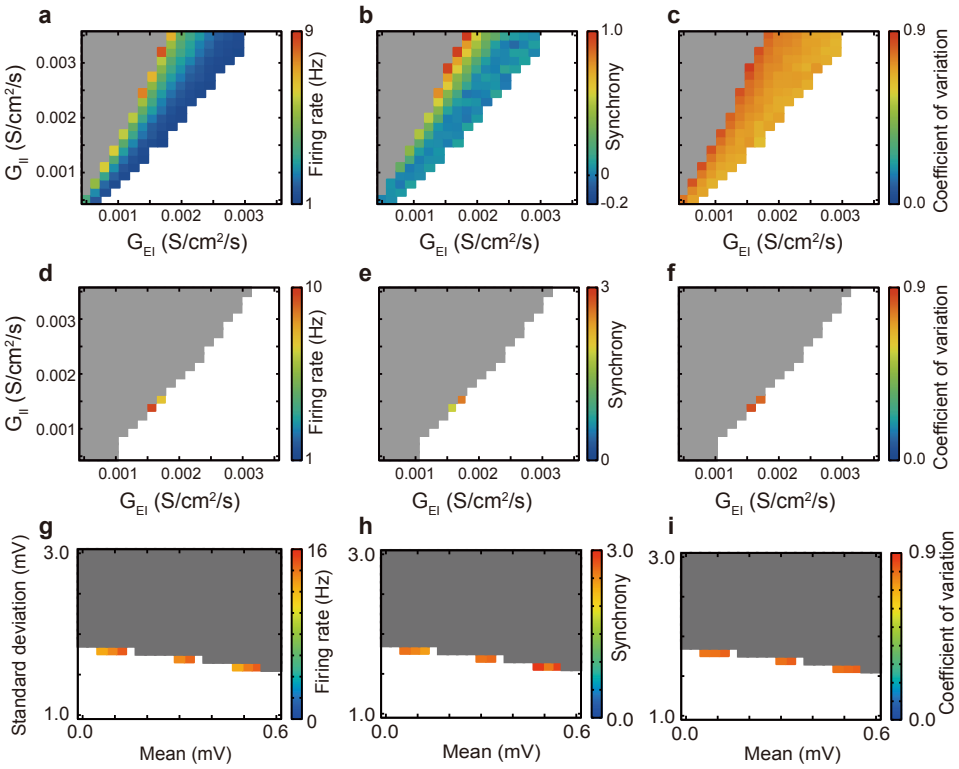

Supplementary Figure 1:

Parameter regions for stable sparse spontaneous activities. (a-c) The firing rate, synchrony measure and CV of low-frequency asynchronous firing are displayed for the SSWD network in the space spanned by inhibitory-to-excitatory and inhibitory-to-inhibitory synaptic weights. An asynchronous firing state does not exist (white area) or shows frequencies > 10 Hz (grey area), for which internal noise is too strong to make spike transmission at strong synapses faithful to their inputs. “Synchrony” is calculated as (c0-r)/r, where c0 and r are the peak and mean of the cross-correlograms averaged over all excitatory neuron pairs. The synchrony measure is zero for perfectly uncorrelated asynchronous firing. (d-f) Similar phase diagrams are shown for the truncated Gaussian-connected network model. Grey area means frequencies > 15 Hz. (g-i) Changing the mean and variance of the truncated Gaussian EPSP distribution does not improve the stability of the sparse spontaneous activity of the truncated Gaussian-connected network.

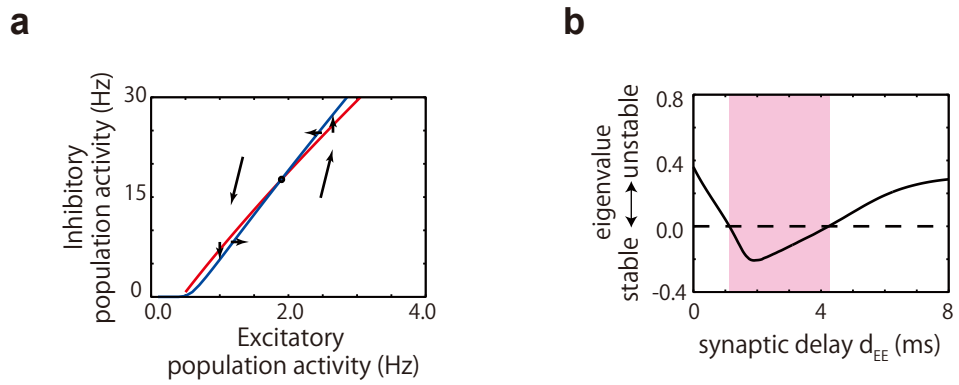

Supplementary Figure 2:

Stability analysis of spontaneous sparse activity in the SSWD neural network. (a) State space portrait of neural population activities was obtained by solving equations (10) and (11) derived in Methods. The intersection (circle) of the nullclines of excitatory (red) and inhibitory (blue) populations represents a steady state. Arrows show the direction of flow on the state space. (b) Negative values of the stability index given by the real part of the eigenvalue in equation (11) indicate that the spontaneous state is stable only in the shaded range of synaptic delay.